Error Analysis of a Dual-parametric Bi-quadratic FEM in Cavitation Computation in Elasticity*

Chunmei Su, Zhiping Li†

LMAM & School of Mathematical Sciences,
Peking University, Beijing 100871, China

Abstract

The orientation preserving conditions and approximation errors of a dual-parametric bi-quadratic finite element method for the computation of both radially symmetric and general nonsymmetric cavity solutions in nonlinear elasticity are analyzed. The analytical results allow us to establish, based on an error equi-distribution principle, an optimal meshing strategy for the method in cavitation computation. Numerical results are in good agreement with the analytical results.

Keywords: error analysis, dual-parametric bi-quadratic finite element, cavitation, optimal meshing strategy

AMS Subject Classification: 65N15, 65N30, 65D05, 74B20, 74G15,74M99

1 Introduction

Void formation on nonlinear elastic bodies under hydrostatic tension was observed and analyzed through a defect model by Gent and Lindley [4]. Ball [2] established a perfect model and studied a class of bifurcation problems in nonlinear elasticity,

*The research was supported by the NSFC project 11171008.

†Corresponding author. Emails: sucm@pku.edu.cn, lizp@math.pku.edu.cn

in which voids form in an intact body so that the total stored energy of the material is minimized in a class of radially symmetric deformations. The work stimulated an intensive study on various aspects of radially symmetric cavitations (see e.g., Sivaloganathan [15], Stuart [21], and a review paper by Horgan and Polignone [6] among many others).

Müller and Spector [12] later developed a general existence theory in nonlinear elasticity that allows for cavitation, which is not necessarily radially symmetric, by adding a surface energy term. Sivaloganathan and Spector [17] deduced the existence of hole creating deformations without the need for the surface energy term under the assumption that the points (a finite number) at which the cavities can form are prescribed. Optimal locations where cavities can arise are also studied analytically [18, 19] and numerically [10].

Numerically computing cavities based on the perfect model of Ball is very challenging, due to the so-called Lavrentiev phenomenon [7]. Though there are numerical methods developed to overcome the Lavrentiev phenomenon in some nonlinear elasticity problems [1, 3, 8, 13, 14], they do not seem to be powerful enough for the cavitation problem. On the other hand, some numerical methods (see e.g., [9, 10, 22]) have been successfully developed for cavitation computation on general domains with single or multiple prescribed defects, based on the defect model or the regularized perfect model [5, 15, 16]. In these models, one considers to minimize the total elastic energy of the form

$$E(u) = \int_{\Omega_\varrho} W(\nabla u(x))dx, \tag{1.1}$$

in a set of admissible functions

$$U = \{u \in W^{1,p}(\Omega_\varrho; \mathbb{R}^n) \text{ is one-to-one a.e. } : u|_{\Gamma_0} = u_0, \det \nabla u > 0 \ a.e.\}, \tag{1.2}$$

where $\Omega_\varrho = \Omega \setminus \bigcup_{i=1}^K B_{\varrho_i}(a_i) \subset \mathbb{R}^n \, (n = 2, 3)$ denotes the region occupied by an elastic body in its reference configuration, $B_{\varrho_i}(a_i) = \{x \in \mathbb{R}^n : |x - a_i| < \varrho_i\}$ are the pre-existing defects of radii ϱ_i centered at a_i, and where in (1.1) $W : M_+^{n\times n} \to \mathbb{R}^+$ is the stored energy density function of the material, $M_+^{n\times n}$ denotes the $n \times n$ matrices with positive determinant, Γ_0 is the boundary of Ω.

The Euler-Lagrange equation of the minimization problem (1.1) is (see [9]):

$$\operatorname{div}(D_F W(\nabla u)) = 0, \qquad \text{in } \Omega_\rho, \tag{1.3}$$

$$D_F W(x, \nabla u)\nu = 0, \qquad \text{on } \cup_{i=1}^{K} \partial B_{\rho_i}(a_i), \tag{1.4}$$

$$u(x) = u_0(x), \qquad \text{on } \Gamma_0. \tag{1.5}$$

A typical class of the stored energy densities considered in the cavitation problem is the polyconvex isotropic functions of the form

$$\begin{aligned} W(F) &= \omega|F|^p + g(\det F) \\ &= \omega(v_1^2 + \cdots + v_n^2)^{p/2} + g(v_1 \cdots v_n), \quad \forall F \in M_+^{n\times n}, \end{aligned} \tag{1.6}$$

where $\omega > 0$ is a material constant, $p \in (n-1, n)$, $v_1, \ldots, v_n$ are the singular values of the deformation gradient F, and $g : (0,\infty) \to (0,\infty)$ is a C^2, strictly convex function satisfying

$$g(\delta) \to +\infty \text{ as } \delta \to 0, \text{ and } \frac{g(\delta)}{\delta} \to +\infty \text{ as } \delta \to +\infty. \tag{1.7}$$

For the energy density of the form (1.6), one has:

$$D_F W(\nabla u) = p\omega\big|\nabla u\big|^{p-2}\nabla u + g'(\det \nabla u)\operatorname{adj} \nabla u^{\mathrm{T}}. \tag{1.8}$$

One of the main difficulties in the computation of the growth of voids is the constraint of orientation preserving, i.e., $\det \nabla u > 0$, for extremely large anisotropic finite element deformations. For the conforming piecewise affine finite element, this requirement demands an unbearably large amount of degrees of freedom ([22]). In [9, 10, 22], other finite element methods are proposed to overcome this difficulty, and these methods have shown significant numerical success in the cavitation computation. In particular, Su and Li [20] analyzed the iso-parametric quadratic finite element method applied in [10], even though limited to the radially symmetric cavitation solutions, the result, the first of its kind to our knowledge, nevertheless quantifies the theoretical as well as practical advantages of the method.

In this paper, we will introduce and analyze a dual-parametric bi-quadratic rectangular finite element method for the cavitation computation, including both radially symmetric and general nonsymmetric voids' growth, and establish a meshing strategy, which is optimal in the sense that the total degrees of freedom is

minimized under certain mild constraints. It turns out that, for the cavitation computation, the dual-parametric bi-quadratic rectangular finite element method is definitely much more efficient than the iso-parametric quadratic triangular finite element method, especially when the prescribed defects are very small. In fact, in the radially symmetric case, the optimal mesh of the new method is essentially solely determined by the approximation accuracy, while the orientation preserving condition plays a leading role in the iso-parametric finite element method in the vicinity of the void.

The structure of the paper is as follows. In § 2, we introduce the dual-parametric bi-quadratic rectangular finite element. § 3 is devoted to deriving the orientation preserving conditions on the mesh distributions. In § 4, we present some results on the interpolation errors of the cavitation solutions. An optimal meshing strategy is established in § 5. Numerical results are presented in § 6. The paper is ended with some concluding remarks in § 7.

2 Dual-parametric bi-quadratic finite element

For simplicity, we restrict ourselves to a simplified problem with $\Omega_\varrho = B_1(0)\setminus B_\varrho(0)$ in $\mathbb{R}^2$. Let $(\hat{T}, \hat{P}, \hat{\Sigma})$ be a standard bi-quadratic rectangular element as shown in Figure 1(a) (here $n = 2$), where $\hat{P} = Q_2(\hat{T})$, $\hat{\Sigma} = \{\hat{p}(\hat{a}_i), 0 \le i \le 8\}$. For a given set of four points $a_i = (R_i\cos\theta_i, R_i\sin\theta_i)$, $0 \le i \le 3$ satisfying $R_0 = R_3 < R_1 = R_2$, $\theta_0 = \theta_1 < \theta_2 = \theta_3$, define $F_T : \hat{T} \to \mathbb{R}^2$ as

$$\begin{cases} R = R_0 + \dfrac{\hat{x}_1 + 1}{2}(R_1 - R_0), \\ \theta = \theta_0 + \dfrac{\hat{x}_2 + 1}{2}(\theta_3 - \theta_0), \\ x_1 = R\cos\theta, x_2 = R\sin\theta. \end{cases} \tag{2.1}$$

It is easily seen that F_T is a injection, thus $T = F_T(\hat{T})$ defines an element. Now define the dual-parametric bi-quadratic finite element (T, P_T, Σ_T) as follows

$$\begin{cases} T = F_T(\hat{T}), \\ P_T = \{p : T \to \mathbb{R}^2 \mid p = \hat{p}\circ F_T^{-1},\ \hat{p} \in \hat{P}\}, \\ \Sigma_T = \{p(a_i), a_i = F_T(\hat{a}_i), 0 \le i \le 8\}. \end{cases} \tag{2.2}$$

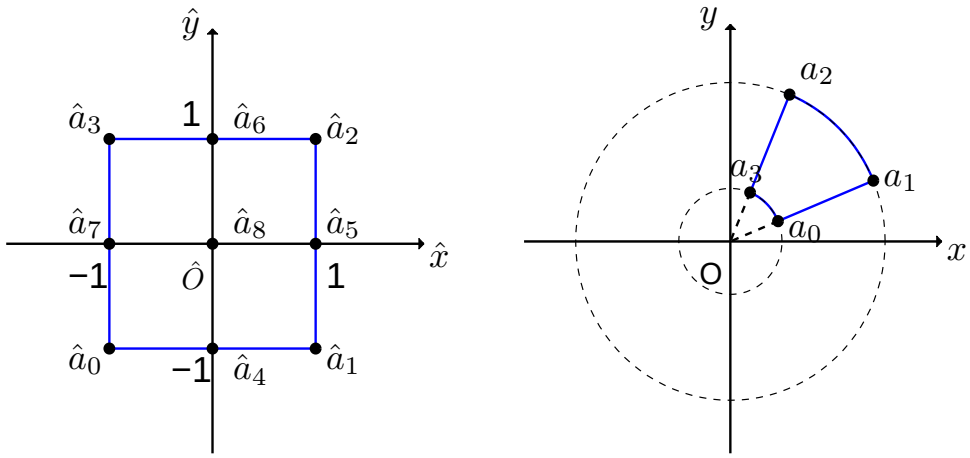

(a) The reference element $\hat{T}$.

(b) An element T in a mesh.

Figure 1: The dual-parametric element.

3 On the orientation preserving conditions

Let $\mathcal{J}$ be a subdivision on $\Omega_{\epsilon_0} = B_1(0) \setminus B_{\epsilon_0}(0)$ as Figure 2(a). A typical curved element in a prescribed circular ring with inner radius ϵ and thickness τ is shown in Figure 2(b). Let N be the number of the evenly spaced elements on each layer, let ϵ and τ represent respectively the inner radius and the thickness of the circular annulus as shown in Figure 2(b). Then, the dual-parametric bi-quadratic finite element function space is given by

$$X_h := \{u_h \in C(\bar{\Omega}_{\epsilon_0}) : u_h|_T \in P_T, u_h(x) = u_0(x), \forall x \in \Gamma_0\},$$

where $\Gamma_0 = \partial B_1(0)$.

We are concerned with orientation preserving of large expansion dominant finite element deformations around a small prescribed void. Without loss of generality, we restrict ourselves to the curved rectangular element as shown in Figure 2(b),

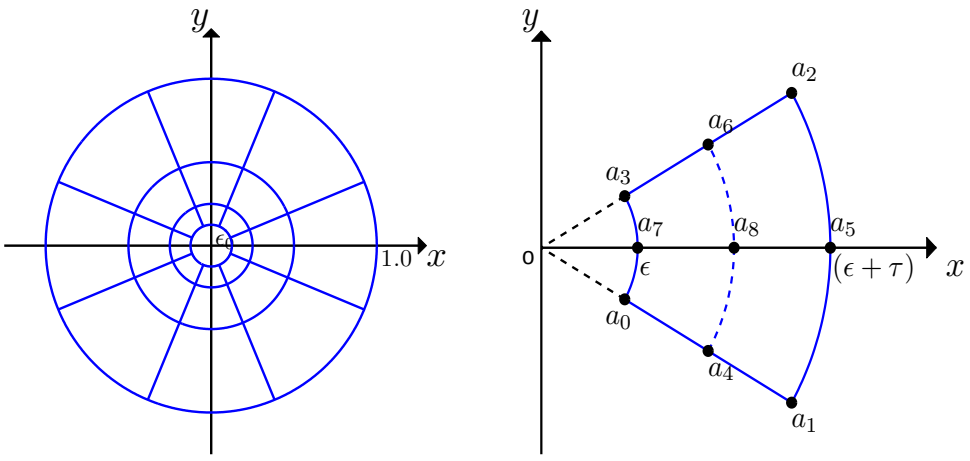

(a) A typical mesh generation in Ω_{ϵ_0}. (b) A typical element in the mesh.

Figure 2: The subdivision of the mesh.

for which F_T can be simplified as

$$\begin{cases} R = \epsilon + \dfrac{\hat{x}_1 + 1}{2}\tau, \\ \theta = \dfrac{\pi}{N}\hat{x}_2, \\ x_1 = R\cos\theta, x_2 = R\sin\theta. \end{cases} \tag{3.1}$$

It is easily verified that $\det \nabla x = \det \frac{\partial F_T}{\partial \hat{x}} = \frac{R\pi\tau}{2N} > 0$.

Let u be the cavitation solution, and let $\mathcal{J}$ be a given mesh (see Figure 2(a)) consisting of well defined curved rectangular elements. To have u be well resolved by functions in the finite element function space defined on $\mathcal{J}$, a necessary condition is that the finite element interpolation function $\Pi u(x)$ is an admissible function, i.e., $\det \nabla \Pi u(x) > 0$ on each of the curved rectangular element. We will investigate in this section the conditions that ensure $\det \nabla \Pi u(x) > 0$ for smooth deformations $u(x) = (u_1(x), u_2(x))$ defined on Ω_{ϵ_0}. Since $\det \nabla \Pi u(x) \cdot \det \nabla x = \det \frac{\partial \Pi u}{\partial \hat{x}}$, it suffices to ensure $\det \frac{\partial \Pi u}{\partial \hat{x}} > 0$. For simplicity, we denote $\Omega_{(\epsilon,\tau)} = \{x : \epsilon \le |x| \le \epsilon + \tau\}$.

Theorem 3.1 *Suppose* $x = (R\cos\theta, R\sin\theta)$, $u(x) = (u_1, u_2) = (r\cos\phi, r\sin\phi)$, *where* $r = r(R,\theta)$, $\phi = \phi(R,\theta)$ *are smooth functions in the domain* $B_1(0) \setminus \{0\}$ *satisfying* $\det \frac{\partial u}{\partial x} \ge c > 0$ *and the derivatives* $\frac{\partial^{i+j} r}{\partial R^i \partial \theta^j}$, $\frac{\partial^{i+j}\phi}{\partial R^i \theta^j}$, $i + j \le 4$, *are bounded, then, there exists a positive constant* $\tau_0 = C_1\epsilon^{1/2}$ *and an integer* $N_0 = C_2\epsilon^{-1/2}$, *such*

that $\det \frac{\partial \Pi u}{\partial x} > 0$ *on the circular annulus* $\Omega_{(\epsilon,\tau)}$ *if* $\tau \le \tau_0$ *and* $N \ge N_0$*, where* C_1*,* C_2 *depend on* c *and* $\|\frac{\partial^3 u_i}{\partial R^3}\|$*,* $\|\frac{\partial^3 u_i}{\partial \theta^3}\|$*,* $\|\frac{\partial^4 u_i}{\partial R^3 \partial \theta}\|$*,* $\|\frac{\partial^4 u_i}{\partial R \partial \theta^3}\|$*. Moreover, the error between the Jacobi determinants of* $\nabla u(x)$ *and* $\nabla \Pi u(x)$ *is given by*

$$\det \frac{\partial \Pi u}{\partial x}(x) = \det \frac{\partial u}{\partial x}(x) + \frac{1}{|x|} O(\tau^2 + N^{-2}). \tag{3.2}$$

Proof. The dual-parametric bi-quadratic finite element interpolation function can be written as

$$\Pi u(x) = \sum_{i=0}^{8} u(a_i) \hat{p}_i(\hat{x}), \tag{3.3}$$

where $\hat{x} = F_T^{-1}(x)$. On the representative element given by (3.1), regarding $u_i(x)$ as the function of R and θ, where $x = (x_1, x_2) = (R\cos\theta, R\sin\theta)$, and Taylor expanding $u_i(a_k)$ at a_8, we obtain

$$\frac{\partial \Pi u}{\partial \hat{x}} = \begin{pmatrix} A_{11} & A_{12} \\ A_{21} & A_{22} \end{pmatrix}, \tag{3.4}$$

where

$$\begin{aligned}
A_{11} &= j_1 \hat{x}_1 \hat{x}_2^2 + \frac{1}{2} b_1 \hat{x}_2^2 + c_1 \hat{x}_1 \hat{x}_2 + d_1 \hat{x}_1 + e_1 \hat{x}_2 + f_1, \\
A_{12} &= j_1 \hat{x}_1^2 \hat{x}_2 + \frac{1}{2} c_1 \hat{x}_1^2 + b_1 \hat{x}_1 \hat{x}_2 + e_1 \hat{x}_1 + g_1 \hat{x}_2 + h_1, \\
A_{21} &= j_2 \hat{x}_1 \hat{x}_2^2 + \frac{1}{2} b_2 \hat{x}_2^2 + c_2 \hat{x}_1 \hat{x}_2 + d_2 \hat{x}_1 + e_2 \hat{x}_2 + f_2, \\
A_{22} &= j_2 \hat{x}_1^2 \hat{x}_2 + \frac{1}{2} c_2 \hat{x}_1^2 + b_2 \hat{x}_1 \hat{x}_2 + e_2 \hat{x}_1 + g_2 \hat{x}_2 + h_2,
\end{aligned}$$

with

$$\begin{aligned}
j_1 = \frac{u_1(a_1) + u_1(a_2) - 2u_1(a_5)}{2} + \frac{u_1(a_0) + u_1(a_3) - 2u_1(a_7)}{2} + 2u_1(a_8) \\
- u_1(a_4) - u_1(a_6) = \frac{\pi^2}{2N^2} \frac{\partial^4 u_1}{\partial R^2 \partial \theta^2}(a_8) \frac{\tau^2}{4} + O(\tau^4 N^{-2} + \tau^2 N^{-4}),
\end{aligned}$$

$$\begin{aligned}
b_1 &= \frac{u_1(a_1) + u_1(a_2) - 2u_1(a_5)}{2} - \frac{u_1(a_0) + u_1(a_3) - 2u_1(a_7)}{2} \\
&= \frac{\pi^2}{N^2} \frac{\partial^3 u_1}{\partial R \partial \theta^2}(a_8) \frac{\tau}{2} + O(\tau^3 N^{-2} + \tau N^{-4}),
\end{aligned}$$

$$
\begin{aligned}
c_1 &= \frac{u_1(a_2)+u_1(a_3)-2u_1(a_6)}{2} - \frac{(u_1(a_0)+u_1(a_1)-2u_1(a_4))}{2} \\
&= \frac{\pi}{N}\frac{\partial^3 u_1}{\partial\theta\partial R^2}(a_8)(\frac{\tau}{2})^2 + O(\tau^4 N^{-1}+\tau^2 N^{-3}), \\
d_1 &= u_1(a_5)+u_1(a_7)-2u_1(a_8) = \frac{\partial^2 u_1}{\partial R^2}(a_8)(\frac{\tau}{2})^2 + O(\tau^4), \\
e_1 &= \frac{u_1(a_2)-u_1(a_1)}{4} - \frac{u_1(a_3)-u_1(a_0)}{4} \\
&= \frac{\pi}{N}\frac{\partial^2 u_1}{\partial R\partial\theta}(a_8)\frac{\tau}{2} + O(\tau^3 N^{-1}+\tau N^{-3}), \\
g_1 &= u_1(a_4)+u_1(a_6)-2u_1(a_8) = \frac{\partial^2 u_1}{\partial\theta^2}(a_8)(\frac{\pi}{N})^2 + O(N^{-4}), \\
f_1 &= \frac{u_1(a_5)-u_1(a_7)}{2} = \frac{\partial u_1}{\partial R}(a_8)\frac{\tau}{2} + \frac{1}{3!}\frac{\partial^3 u_1}{\partial R^3}(a_8)(\frac{\tau}{2})^3 + O(\tau^5), \\
h_1 &= \frac{u_1(a_6)-u_1(a_4)}{2} = \frac{\partial u_1}{\partial\theta}(a_8)\frac{\pi}{N} + \frac{1}{3!}\frac{\partial^3 u_1}{\partial\theta^3}(a_8)(\frac{\pi}{N})^3 + O(N^{-5}),
\end{aligned}
$$

and j_2, $b_2, \cdots, h_2$ have the similar formulae as above with only u_1 replaced by u_2. It follows that

$$
\begin{aligned}
A_{11} &= \frac{\partial u_1}{\partial R}(a_8)\frac{\tau}{2} + \frac{\partial^2 u_1}{\partial R^2}(a_8)(\frac{\tau}{2})^2\hat{x}_1 + \frac{\partial^2 u_1}{\partial R\partial\theta}(a_8)\frac{\tau}{2}\frac{\pi}{N}\hat{x}_2 + \frac{\partial^3 u_1}{\partial R^2\partial\theta}(a_8)(\frac{\tau}{2})^2\frac{\pi}{N}\hat{x}_1\hat{x}_2 \\
&\quad + \frac{1}{2}\frac{\partial^3 u_1}{\partial R\partial\theta^2}(a_8)\frac{\tau}{2}(\frac{\pi}{N})^2\hat{x}_2^2 + \frac{1}{2}\frac{\partial^4 u_1}{\partial R^2\partial\theta^2}(a_8)(\frac{\tau}{2})^2(\frac{\pi}{N})^2\hat{x}_1\hat{x}_2^2 + O(\tau^3+\tau N^{-3}) \\
&= \frac{\tau}{2}\frac{\partial u_1}{\partial R}(x) + O(\tau^3+\tau N^{-3}), \qquad (3.5)
\end{aligned}
$$

where $x = F_T(\hat{x})$. Similarly,

$$
\begin{aligned}
A_{12} &= \frac{\partial u_1}{\partial\theta}(a_8)\frac{\pi}{N} + \frac{\partial^2 u_1}{\partial R\partial\theta}(a_8)\frac{\tau}{2}\frac{\pi}{N}\hat{x}_1 + \frac{\partial^2 u_1}{\partial\theta^2}(a_8)(\frac{\pi}{N})^2\hat{x}_2 + \frac{\partial^3 u_1}{\partial R\partial\theta^2}\frac{\tau}{2}(\frac{\pi}{N})^2(a_8)\hat{x}_1\hat{x}_2 \\
&\quad + \frac{1}{2}\frac{\partial^3 u_1}{\partial R^2\partial\theta}(a_8)(\frac{\tau}{2})^2\frac{\pi}{N}\hat{x}_1^2 + \frac{1}{2}\frac{\partial^4 u_1}{\partial R^2\partial\theta^2}(a_8)(\frac{\tau}{2})^2(\frac{\pi}{N})^2\hat{x}_1^2\hat{x}_2 + O(\tau^3+\tau N^{-3}) \\
&= \frac{\pi}{N}\frac{\partial u_1}{\partial\theta}(x) + O(N^{-3}+\tau^3 N^{-1}), \qquad (3.6) \\
A_{21} &= \frac{\tau}{2}\frac{\partial u_2}{\partial R}(x) + O(\tau^3+\tau N^{-3}), \qquad (3.7) \\
A_{22} &= \frac{\pi}{N}\frac{\partial u_2}{\partial\theta}(x) + O(N^{-3}+\tau^3 N^{-1}), \qquad (3.8)
\end{aligned}
$$

where the constant in $O(\cdot)$ depends on $\|\frac{\partial^3 u_i}{\partial R^3}\|$, $\|\frac{\partial^3 u_i}{\partial\theta^3}\|$, $\|\frac{\partial^4 u_i}{\partial R^3\partial\theta}\|$, $\|\frac{\partial^4 u_i}{\partial R\partial\theta^3}\|$. Thus

$$
\det\frac{\partial\Pi u}{\partial\hat{x}}(\hat{x}_1,\hat{x}_2) = \frac{\tau}{2}\frac{\pi}{N}\Big(\frac{\partial u_1}{\partial R}\frac{\partial u_2}{\partial\theta} - \frac{\partial u_2}{\partial R}\frac{\partial u_1}{\partial\theta}\Big)\Big|_x + O(\tau^3 N^{-1}+\tau N^{-3}). \qquad (3.9)
$$

Noticing that $R \geq \epsilon$ and

$$\frac{\partial u_1}{\partial R}\frac{\partial u_2}{\partial \theta} - \frac{\partial u_1}{\partial \theta}\frac{\partial u_2}{\partial R} = R\Big(\frac{\partial u_1}{\partial x_1}\frac{\partial u_2}{\partial x_2} - \frac{\partial u_1}{\partial x_2}\frac{\partial u_2}{\partial x_1}\Big) = R\det\frac{\partial u}{\partial x},$$

which yields the first part of the conclusion. (3.2) is a direct consequence of (3.9) and the fact that $\det\frac{\partial x}{\partial \hat{x}} = \frac{R\tau}{2}\frac{\pi}{N}$. ■

Remark 3.2 *As a consequence of Theorem 3.1, we see that, for a general cavity deformation, the interpolation function is orientation preserving on a mesh* $\Omega_{\epsilon_0} = \bigcup_{i=0}^{m} \Omega_{(\epsilon_i,\tau_i)}$, *where* $\epsilon_{i+1} = \epsilon_i + \tau_i$, *which satisfies* $\tau_i \leq C_1\sqrt{\epsilon_i}$ *and* $N_i \geq C_2\epsilon_i^{-1/2}$ *for some constants* C_1 *and* C_2. *If restricted to a radially symmetric cavity deformation, we may expect to have a more relaxed orientation preserving condition.*

Theorem 3.3 *For a radially symmetric deformation* $u(x) = \frac{r(R)}{R}x$, *where* $r > 0$ *is an increasing convex function satisfying*

$$4r(\epsilon + \tau/2) \geq 3r(\epsilon) + r(\epsilon + \tau), \tag{3.10}$$

then the interpolation function $\Pi u(x)$ *preserves orientation on the circular ring* $\Omega_{(\epsilon,\tau)}$. *Moreover, if*

$$0 < m \leq \det\frac{\partial u}{\partial x}(x) = \frac{r(R)r'(R)}{R} \leq M, \tag{3.11}$$

where $R = |x|$, *then*

$$\det\frac{\partial \Pi u}{\partial x}(x) = \det\frac{\partial u}{\partial x}(x) + O(N^{-2}) + \frac{1}{|x|}O(\tau^2). \tag{3.12}$$

Proof. For $u(x) = \frac{r(R)}{R}x$, a direct but tedious calculation yields

$$\Pi u(x) = (X_1, X_2)^T = C(\hat{x}_1)\big(1 - 2\hat{x}_2^2\sin\frac{\pi}{2N}, \hat{x}_2\sin\frac{\pi}{N}\big)^T, \tag{3.13}$$

where

$$C(\hat{x}_1) = \frac{1}{2}\hat{x}_1(\hat{x}_1 - 1)r(\epsilon) + \frac{1}{2}\hat{x}_1(\hat{x}_1 + 1)r(\epsilon + \tau) + (1 - \hat{x}_1^2)r(\epsilon + \tau/2). \tag{3.14}$$

Hence

$$\det\frac{\partial \Pi u}{\partial \hat{x}} = C(\hat{x}_1)C'(\hat{x}_1)\sin\frac{\pi}{N}\big(1 + 2\hat{x}_2^2\sin^2\frac{\pi}{2N}\big).$$

Since $r(R)$ is increasing and convex, it is easily seen that $C(\hat{x}_1) > 0$ on $[-1, 1]$. On the other hand, $C'(\hat{x}_1) = (\hat{x}_1 - \frac{1}{2})r(\epsilon) + (\hat{x}_1 + \frac{1}{2})r(\epsilon + \tau) - 2\hat{x}_1 r(\epsilon + \tau/2)$ is a linear function of $\hat{x}_1$ with $C'(1) = \frac{1}{2}(r(\epsilon) + 3r(\epsilon + \tau) - 4r(\epsilon + \tau/2)) > 0$, and $C'(-1) = \frac{1}{2}(4r(\epsilon + \tau/2) - 3r(\epsilon) - r(\epsilon + \tau)) > 0$, thus $C'(\hat{x}_1) > 0$ on $[-1, 1]$. Hence, the first part of the theorem follows.

Taylor expanding $r(\epsilon)$, $r(\epsilon + \tau/2)$, $r(\epsilon + \tau)$ at $R = \epsilon + \frac{\hat{x}_1+1}{2}\tau$, one gets

$$C(\hat{x}_1) = r(R) + O(\tau^3), \quad C'(\hat{x}_1) = \frac{r'(R)\tau}{2} + O(\tau^3).$$

Thus, it follows from $\det(\frac{\partial \Pi u}{\partial x}\frac{\partial x}{\partial \hat{x}}) = \det \frac{\partial \Pi u}{\partial \hat{x}}$ and $\det \frac{\partial x}{\partial \hat{x}} = \frac{R\tau}{2}\frac{\pi}{N}$ that

$$\begin{aligned} \det \frac{\partial \Pi u}{\partial x} &= \frac{2C(\hat{x}_1)C'(\hat{x}_1)}{R\tau}(1 + O(N^{-2})) \\ &= \frac{(r(R) + O(\tau^3))(r'(R) + O(\tau^2))}{R}(1 + O(N^{-2})) \\ &= \frac{r(R)r'(R)}{R} + \frac{O(\tau^2)}{R} + O(N^{-2}), \end{aligned}$$

which gives (3.12) and completes the proof of the theorem. ■

Remark 3.4 *For the energy minimizers among radially symmetric cavity deformations, the condition* (3.11) *in Theorem 3.3 is generally satisfied, and there exists a positive constant C such that* (3.10) *holds whenever $\epsilon \geq C\tau^2$ (see [20]). As a consequence, we see that, for the dual-parametric bi-quadratic finite element method, the orientation preserving adds no further restriction on the number of elements N on an annular ring, which means much less total degrees of freedom is required as compared with the methods in [20, 22].*

4 Interpolation errors of cavity deformations

In this section, the interpolation errors are estimated, including those on the interpolation function and the elastic energy in the dual-parametric bi-quadratic finite element function spaces defined on the meshes described in § 3. Throughout this section, $u(x)$ is supposed to be a smooth cavitation deformation in the regularized domain Ω_{ϵ_0}. We also assume that the meshes are so given that Theorem 3.1 holds.

4.1 The error of the interpolation function

Let $\hat{x} = F_T^{-1}(x) \in \hat{T}$, where $x \in T$ is a point on the mesh. We will estimate, in this subsection, the errors between $u(x)$ and its interpolation function $\Pi u(x)$.

Theorem 4.1 *Under the assumption of Theorem 3.1, the error between a cavity deformation $u(x)$ and its interpolation function $\Pi u(x)$ satisfies*

$$\|u(x) - \Pi u(x)\| = O(\tau^3 + N^{-3}). \tag{4.1}$$

Proof. For a typical element as used in § 3, denote $X = \Pi u(x) = (X_1, X_2)$, where $x = F_T(\hat{x})$. With the same notation as used in Theorem 3.1, and Taylor expanding $u_i(a_k)$ at a_8, one gets

$$\begin{aligned}
X_1 &= \sum_{i=0}^{8} u_1(a_i)\hat{p}_i(\hat{x}) \\
&= u_1(a_8) + f_1\hat{x}_1 + h_1\hat{x}_2 + \frac{d_1}{2}\hat{x}_1^2 + e_1\hat{x}_1\hat{x}_2 + \frac{g_1}{2}\hat{x}_2^2 + \frac{b_1}{2}\hat{x}_1\hat{x}_2^2 + \frac{c_1}{2}\hat{x}_1^2\hat{x}_2 + \frac{j_1}{2}\hat{x}_1^2\hat{x}_2^2 \\
&= u_1(a_8) + \frac{\partial u_1}{\partial R}(a_8)\frac{\tau}{2}\hat{x}_1 + \frac{\partial u_1}{\partial \theta}(a_8)\frac{\pi}{N}\hat{x}_2 + \frac{1}{2}\frac{\partial^2 u_1}{\partial R^2}(a_8)(\frac{\tau}{2})^2\hat{x}_1^2 \\
&\quad + \frac{\partial^2 u_1}{\partial R\partial\theta}(a_8)\frac{\tau}{2}\frac{\pi}{N}\hat{x}_1\hat{x}_2 + \frac{1}{2}\frac{\partial^2 u_1}{\partial \theta^2}(a_8)(\frac{\pi}{N})^2\hat{x}_2^2 + \frac{1}{2}\frac{\partial^3 u_1}{\partial R\partial\theta^2}(a_8)\frac{\tau}{2}(\frac{\pi}{N})^2\hat{x}_1\hat{x}_2^2 \\
&\quad + \frac{1}{2}\frac{\partial^3 u_1}{\partial R^2\partial\theta}(a_8)(\frac{\tau}{2})^2\frac{\pi}{N}\hat{x}_1^2\hat{x}_2 + \frac{1}{2}\frac{\partial^4 u_1}{\partial R^2\partial\theta^2}(a_8)(\frac{\tau}{2})^2(\frac{\pi}{N})^2\hat{x}_1^2\hat{x}_2^2 + O(\tau^3 + N^{-3}) \\
&= u_1(x) + O(\tau^3 + N^{-3}).
\end{aligned}$$

Similarly, $X_2 = u_2(x) + O(\tau^3 + N^{-3})$. Hence, the conclusion follows. ■

Theorem 4.2 *Denote $\Omega_{\epsilon_0} = \bigcup_{i=0}^{m} \Omega_{(\epsilon_i,\tau_i)}$, where $\Omega_{(\epsilon,\tau)} = \{x : \epsilon \le |x| \le \epsilon + \tau\}$, $\epsilon_{i+1} = \epsilon_i + \tau_i$, $\epsilon_{m+1} = 1.0$. Let N_i be the number of elements in the layer $\Omega_{(\epsilon_i,\tau_i)}$. If ϵ_i, τ_i, N_i satisfy the assumptions of Theorem 3.1, and $\tau_i = O(h)$, $N_i^{-1} = O(h)$, as $h \to 0$, then the error between a cavity deformation $u(x)$ and its interpolation function Πu satisfies*

$$\|u(x) - \Pi u(x)\|_{1,p} = O(h^2). \tag{4.2}$$

Proof. On a representative element as shown in Figure 2(b), by (3.1), (3.4) and $\frac{\partial \Pi u}{\partial x}\frac{\partial x}{\partial \hat{x}} = \frac{\partial \Pi u}{\partial \hat{x}}$, we have

$$\frac{\partial \Pi u(x)}{\partial x} = \frac{2N}{\pi R\tau}\begin{pmatrix} A_{11}R\frac{\pi}{N}\cos\theta - A_{12}\frac{\tau}{2}\sin\theta & A_{11}R\frac{\pi}{N}\sin\theta + A_{12}\frac{\tau}{2}\cos\theta \\ A_{21}R\frac{\pi}{N}\cos\theta - A_{22}\frac{\tau}{2}\sin\theta & A_{21}R\frac{\pi}{N}\sin\theta + A_{22}\frac{\tau}{2}\cos\theta \end{pmatrix}, \quad (4.3)$$

where A_{ij} are given by (3.5)-(3.8). Denote

$$\frac{\partial \Pi u(x)}{\partial x} - \frac{\partial u}{\partial x} = \begin{pmatrix} B_{11} & B_{12} \\ B_{21} & B_{22} \end{pmatrix}.$$

Then, it follows from (4.3), (3.5) and (3.6) that

$$\begin{aligned} B_{11} &= \frac{2N}{\pi R\tau}(A_{11}R\frac{\pi}{N}\cos\theta - A_{12}\frac{\tau}{2}\sin\theta) - \frac{\partial u_1}{\partial R}\cos\theta + \frac{\partial u_1}{\partial \theta}\frac{\sin\theta}{R} \\ &= O(\tau^2 + N^{-3}) + \frac{1}{R}O(\tau^3 + N^{-2}). \end{aligned}$$

Since $\tau = O(h)$, $N^{-1} = O(h)$, this yields $B_{11} = \frac{1}{R}O(h^2)$, similarly, $B_{ij} = \frac{1}{R}O(h^2)$. As a consequence $|\frac{\partial \Pi u}{\partial x} - \frac{\partial u}{\partial x}|^p = \frac{1}{R^p}O(h^{2p})$. Thus $\|\frac{\partial \Pi u}{\partial x} - \frac{\partial u}{\partial x}\|_p = (\int_{\epsilon_0}^1 R^{1-p}dR)^{\frac{1}{p}}O(h^2)$, which completes the proof, since $1 < p < 2$. ■

4.2 The error on the elastic energy

Let $\mathcal{J}(\Omega_{(\epsilon,\tau)})$ be a dual-parametric bi-quadratic finite element division of $\Omega_{(\epsilon,\tau)}$ consisting of only one layer of evenly distributed elements, denoted by T_j, $j = 1, \cdots, N$. For the energy density function of the form (1.6), denote

$$E_1(u;\Omega_{(\epsilon,\tau)}) = \int_{\Omega_{(\epsilon,\tau)}} \omega \left|\frac{\partial u}{\partial x}\right|^p dx, \quad (4.4)$$

$$E_2(u;\Omega_{(\epsilon,\tau)}) = \int_{\Omega_{(\epsilon,\tau)}} g\left(\det \frac{\partial u}{\partial x}\right) dx, \quad (4.5)$$

$$A(\epsilon,\tau) = (2-p)\int_{\epsilon}^{\epsilon+\tau} R^{1-p}dR = (\epsilon+\tau)^{2-p} - \epsilon^{2-p}, \quad (4.6)$$

and let $err(E_i(\Pi u;\Omega_{(\epsilon,\tau)})) = |E_i(\Pi u;\Omega_{(\epsilon,\tau)}) - E_i(u;\Omega_{(\epsilon,\tau)})|$ be the absolute interpolation error of $E_i(u;\Omega_{(\epsilon,\tau)}))$, $i = 1, 2$, respectively. We have the following result.

Theorem 4.3 *Under the assumption of Theorem 3.1, the elastic energy of a cavity deformation $u(x)$ and its interpolation function Πu satisfy*

$$E_1(u;\Omega_{(\epsilon,\tau)}) = O(A(\epsilon,\tau)), \quad E(u;\Omega_{(\epsilon,\tau)}) = O(A(\epsilon,\tau)), \tag{4.7}$$

$$err(E_1(\Pi u;\Omega_{(\epsilon,\tau)})) = A(\epsilon,\tau)O(\tau^2+N^{-2}), \tag{4.8}$$

$$err(E_2(\Pi u;\Omega_{(\epsilon,\tau)})) = O(\tau^3+\tau N^{-2}), \tag{4.9}$$

$$err(E(\Pi u;\Omega_{(\epsilon,\tau)})) = A(\epsilon,\tau)O(\tau^2+N^{-2}), \tag{4.10}$$

where $A(\epsilon,\tau)$ is defined as (4.6). Moreover, if there exist positive constants $0 < c \le C$ such that $c \le |\frac{\partial u}{\partial \theta}| \le C$, then

$$E_1(u;\Omega_{(\epsilon,\tau)}) \sim A(\epsilon,\tau), \quad E(u;\Omega_{(\epsilon,\tau)}) \sim A(\epsilon,\tau), \tag{4.11}$$

$$err(E_1(\Pi u;\Omega_{(\epsilon,\tau)})) = E_1(u;\Omega_{(\epsilon,\tau)})O(\tau^2+N^{-2}), \tag{4.12}$$

$$err(E(\Pi u;\Omega_{(\epsilon,\tau)})) = E(u;\Omega_{(\epsilon,\tau)})O(\tau^2+N^{-2}). \tag{4.13}$$

Proof. Since $\frac{\partial u_i}{\partial R}$, $\frac{\partial u_i}{\partial \theta}$ are bounded, it follows that $|\frac{\partial u}{\partial x}(x)|^p = O(R^{-p})$. Thus $E_1(u;\Omega_{(\epsilon,\tau)}) = O(\int_\epsilon^{\epsilon+\tau} R^{1-p}dR) = O(A(\epsilon,\tau))$. Noticing that g is bounded and $A(\epsilon,\tau) > (2-p)\tau$, then $E_2(u;\Omega_{(\epsilon,\tau)}) = O(\tau) = O(A(\epsilon,\tau))$, so that we deduce (4.7). In view of (4.3), we find that

$$\begin{aligned}
\left|\frac{\partial \Pi u}{\partial x}\right|^2 &= \frac{4}{\tau^2}(A_{11}^2+A_{21}^2)+\frac{N^2}{\pi^2R^2}(A_{12}^2+A_{22}^2)\\
&= \left(\frac{\partial u_1}{\partial R}(x)\right)^2+\left(\frac{\partial u_2}{\partial R}(x)\right)^2+\frac{1}{R^2}\left(\left(\frac{\partial u_1}{\partial \theta}(x)\right)^2+\left(\frac{\partial u_2}{\partial \theta}(x)\right)^2\right)\\
&\quad +\sum_{i=1}^2\left|\frac{\partial u_i}{\partial R}\right|O(\tau^2+N^{-3})+\frac{1}{R^2}\sum_{i=1}^2\left|\frac{\partial u_i}{\partial \theta}\right|O(\tau^3+N^{-2})\\
&= \left|\frac{\partial u}{\partial x}\right|^2+\sum_{i=1}^2\left|\frac{\partial u_i}{\partial R}\right|O(\tau^2+N^{-3})+\frac{1}{R^2}\sum_{i=1}^2\left|\frac{\partial u_i}{\partial \theta}\right|O(\tau^3+N^{-2}).
\end{aligned}$$

Since $\frac{\partial u_i}{\partial R}$ is bounded and $|\frac{\partial u}{\partial x}| \ge \frac{1}{R}|\frac{\partial u_i}{\partial \theta}|$, this implies

$$\begin{aligned}
\left|\frac{\partial \Pi u}{\partial x}\right|^p &= \left|\frac{\partial u}{\partial x}\right|^p(1+O(\tau^2+N^{-3}))+\left|\frac{\partial u}{\partial x}\right|^{p-2}\frac{1}{R^2}\sum_{i=1}^2|\frac{\partial u_i}{\partial \theta}|O(\tau^3+N^{-2})\\
&= \left|\frac{\partial u}{\partial x}\right|^p(1+O(\tau^2+N^{-3}))+\left|\frac{\partial u}{\partial x}\right|^{p-1}\frac{1}{R}O(\tau^3+N^{-2}).
\end{aligned}$$

Obviously, the first term will lead to a relative error of the order $O(\tau^2 + N^{-3})$ to the first part of the energy E_1. What remains to consider is the second term. Applying the Hölder inequality, we deduce that

$$\int_T \Big|\frac{\partial u}{\partial x}\Big|^{p-1}\frac{1}{R}dx \le \Big(\int_T \Big|\frac{\partial u}{\partial x}\Big|^p dx\Big)^{1-\frac{1}{p}}\Big(\int_T R^{-p}dx\Big)^{\frac{1}{p}} = \Big(\frac{2\pi A(\epsilon,\tau)}{N(2-p)}\Big)^{\frac{1}{p}}\Big(\int_T \Big|\frac{\partial u}{\partial x}\Big|^p dx\Big)^{1-\frac{1}{p}}.$$

Applying the Hölder inequality again yields

$$\sum_{j=1}^{N}\int_{T_j}\Big|\frac{\partial u}{\partial x}\Big|^{p-1}\frac{1}{R}dx \le (\frac{2\pi}{2-p}A(\epsilon,\tau))^{1/p}E_1(u;\Omega_{(\epsilon,\tau)})^{1-1/p}\omega^{1/p-1}.$$

Hence, we obtain

$$E_1(\Pi u;\Omega_{(\epsilon,\tau)}) = E_1(u;\Omega_{(\epsilon,\tau)})(1+O(\tau^2+N^{-3}))+E_1(u;\Omega_{(\epsilon,\tau)})^{1-\frac{1}{p}}A(\epsilon,\tau)^{\frac{1}{p}}O(\tau^3+N^{-2}),$$

which together with (4.7) yields (4.8).

On the other hand, by (3.2) and the fact that g is strictly convex,

$$\begin{aligned} E_2(\Pi u;\Omega_{(\epsilon,\tau)}) &= \sum_{j=1}^{N}\int_{T_j} g(\det\nabla u)dx + \sum_{j=1}^{N}\int_{T_j} g'(\eta_x)|x|^{-1}dx\,O(\tau^2+N^{-2}) \\ &= E_2(u;\Omega_{(\epsilon,\tau)}) + \sum_{j=1}^{N}\int_{T_j}|x|^{-1}dx\,O(\tau^2+N^{-2}) \\ &= E_2(u;\Omega_{(\epsilon,\tau)}) + O(\tau^3+\tau N^{-2}). \end{aligned} \tag{4.14}$$

(4.10) is a direct consequence of (4.8), (4.9) and $A(\epsilon,\tau) > (2-p)\tau$, for $\epsilon \in [0, 1-\tau]$.

Finally, if there exists a positive constant $c > 0$ such that $\sum_{i=1}^{2}(\frac{\partial u_i}{\partial\theta})^2 \ge c$ and thus $|\frac{\partial u}{\partial x}(x)|^p \sim R^{-p}$, meaning that there exist positive constants C_1 and C_2 such that $C_1R^{-p} \le |\frac{\partial u}{\partial x}(x)|^p \le C_2R^{-p}$, this gives (4.11). This together with (4.8) and (4.10) yield (4.12) and (4.13). ■

Theorem 4.4 *For the radially symmetric cavity solution, the error of the energy satisfies* $E(\Pi u;\Omega_{(\epsilon,\tau)}) = E(u;\Omega_{(\epsilon,\tau)})(1+O(\max\{\epsilon,\tau\}^{p-1}\tau^2+N^{-2}))$.

Proof. For the radially symmetric solution, it follows from (3.13) that

$$\frac{\partial\Pi u}{\partial\hat{x}} = \begin{pmatrix} C'(\hat{x}_1)(1-2\hat{x}_2^2\sin^2\frac{\pi}{2N}) & -4C(\hat{x}_1)\hat{x}_2\sin^2\frac{\pi}{2N} \\ C'(\hat{x}_1)\hat{x}_2\sin\frac{\pi}{N} & C(\hat{x}_1)\sin\frac{\pi}{N}. \end{pmatrix}$$

Thus, by (3.14) and the facts that $r(R) \geq r(0) > 0$ and $r'(R) \leq MR$, one gets

$$\begin{aligned}
\left|\frac{\partial \Pi u}{\partial x}\right|^2 &= \frac{4}{\tau^2} C'(\hat{x}_1)^2 (1 + O(N^{-4})) + \frac{N^2}{\pi^2 R^2} C(\hat{x}_1)^2 \sin^2 \frac{\pi}{N} (1 + O(N^{-2})) \\
&= (r'(R) + O(\tau^2))^2 (1 + O(N^{-4})) + \frac{(r(R) + O(\tau^3))^2}{R^2} (1 + O(N^{-2})) \\
&= \frac{r(R)^2}{R^2} (1 + O(\tau^3 + N^{-2})) + r'(R)^2 + r'(R) O(\tau^2) \\
&= (r'(R)^2 + \frac{r(R)^2}{R^2})(1 + O(\tau^3 + N^{-2} + r'(R) R^2 \tau^2)) \\
&= (r'(R)^2 + \frac{r(R)^2}{R^2})(1 + O(\tau^3 + N^{-2} + (\epsilon + \tau)^3 \tau^2)).
\end{aligned}$$

It follows that

$$E_1(\Pi u; \Omega_{(\epsilon,\tau)}) = E_1(u; \Omega_{(\epsilon,\tau)})(1 + O(\epsilon^3 \tau^2 + \tau^3 + N^{-2})).$$

On the other hand, by (3.12) and with similar arguments as in the proof of Theorem 4.3 (see (4.14)), one has that

$$E_2(\Pi u; \Omega_{(\epsilon,\tau)}) = E_2(u; \Omega_{(\epsilon,\tau)}) + O(\tau^3 + (\epsilon + \tau)\tau N^{-2}).$$

Recalling that

$$E_1(u; \Omega_{(\epsilon,\tau)}) = 2\pi \int_{\epsilon}^{\epsilon+\tau} (r'(R)^2 + \frac{r(R)^2}{R^2})^{p/2} R dR \sim A(\epsilon, \tau) > (2 - p)\tau,$$

we obtain

$$\begin{aligned}
err(E_2(\Pi u; \Omega_{(\epsilon,\tau)}) &= E_1(u; \Omega_{(\epsilon,\tau)}) \frac{O(\tau^3 + (\epsilon + \tau)\tau N^{-2})}{A(\epsilon, \tau)} \\
&= O(\max\{\epsilon, \tau\}^{p-1} \tau^2 + (\epsilon + \tau) N^{-2}),
\end{aligned}$$

which completes the proof. ■

5 A meshing strategy

The aim of this section is to establish, for a given reference mesh size $h > 0$, a meshing strategy on the domain $\Omega_{\epsilon_0} = B_1(0) \setminus B_{\epsilon_0}(0)$, *i.e.* to design a method of calculating ϵ_i, τ_i, N_i, where $\epsilon_{i+1} = \epsilon_i + \tau_i$, and N_i is the number of the elements in the layer $\Omega_{(\epsilon_i \tau_i)}$, so that, on $\Omega_{\epsilon_0} = \bigcup_{i=0}^{m} \Omega_{(\epsilon_i, \tau_i)}$, a cavity solution u and its finite element interpolation function Πu satisfy

(C1) the orientation preserving condition: $\det \nabla \Pi u > 0$;

(C2) the approximation condition: $\|u - \Pi u\|_{1,p} = O(h^2)$;

(C3) error sub-equi-distribution condition (see (4.11)-(4.13)): $A(\epsilon_i, \tau_i) = O(h)$;

(C4) least total degrees of freedom condition: $N_d = \sum_{i=0}^{m} N_i$ is minimized under the restriction that $N_{i+1} = N_i$ or $N_{i+1} = 2N_i$.

By Theorem 3.1, for a radially symmetric cavity solution, the condition C1 can be assured by setting $\tau_i \le C_1 \epsilon_i^{1/2}$, while in nonsymmetric case, setting in addition $N_i \ge C_2 \epsilon_i^{-1/2}$ meets the requirement. By Theorem 4.2, a sufficient condition for the condition C2 to hold is $N_i^{-1} = O(h), \tau_i = O(h)$.

The idea of error equi-distribution is often used in mesh adaptivity and mesh redistribution. By Theorem 4.3, $A(\epsilon_i, \tau_i)$ can serve as a monitor for the energy error equi-distribution, especially in the neighborhood of the void. Without loss of generality, assume $\epsilon_m > \frac{1}{2}$, since $\epsilon_m + \tau_m = 1$ for the layer m, this implies $A(\epsilon_m, \tau_m) = 1 - (1 - \tau_m)^{2-p} \le (2-p)2^{p-1}\tau_m$. Thus, it is easily verified that, for a given constant $C \ge (2-p)2^{p-1}$, a reference mesh size $0 < h \le h_0 \le \frac{2-p}{2^{2-p}C}$, $A(\epsilon_m, \tau_m) \le Ch$, provided that $\tau_m \le \frac{C}{(2-p)2^{p-1}}h$. Hence, it is natural to require C3: $A(\epsilon_i, \tau_i) \le Ch$, for all $0 \le i \le m$, which imposes an implicit condition on the layer's thickness τ_i. In fact, given $C \ge (2-p)2^{p-1}$ and $h_0 \ge h > 0$, denoting $d(x,h) = (x^{2-p} + Ch)^{\frac{1}{2-p}} - x$, we have $A(x, d(x,h)) = Ch$. On the other hand, since $p \in (1,2)$, we have $Ch = A(\epsilon_i, d(\epsilon_i, h)) \triangleq (2-p)\int_{\epsilon_i}^{\epsilon_i + d(\epsilon_i,h)} R^{1-p} dR \ge \frac{(2-p)d(\epsilon_i,h)}{(1+d(\epsilon_i,h))^{p-1}}$, which implies that $d(\epsilon_i, h) \le 1$, as long as $0 < h \le h_1 \le \frac{2-p}{2^{p-1}C}$, and consequently $\frac{(2-p)d(\epsilon_i,h)}{(1+d(\epsilon_i,h))^{p-1}} \le Ch$ yields $d(\epsilon_i, h) \le \frac{2^{p-1}C}{(2-p)}h$. Thus, for the condition C3 and $\tau_i = O(h)$ to hold, it suffices to require $\tau_i \le d(\epsilon_i, h)$.

Finally, assuming an optimized distribution of layers is given, then, the condition C4 can be achieved easily by taking the least admissible N_i, $0 \le i \le m$. It is in this sense that the total degrees of freedom are minimized.

For given positive constants C_1, C_2, $C \ge (2-p)2^{p-1}$, $h \le \min\{h_0, h_1\}$, $A_1 < A_2$ satisfying $[(A_2 h)^{-1}, (A_1 h)^{-1}] \cap \mathbb{Z}_+ \ne \emptyset$, the analysis above leads to the following meshing strategy satisfying C1-C4 for non-radially-symmetric cavitaty solutions.

A meshing strategy of $\{\Omega_{(\epsilon_i,\tau_i)}\}_{i=0}^m$:

(1) Take $\tilde{N}_m \in [(A_2h)^{-1}, (A_1h)^{-1}] \cap \mathbb{Z}_+$. Let $\bar{N}_0 = \min\{N \in \mathbb{Z}_+ : N \geq C_2\epsilon_0^{-1/2}\}$. Set $k = \min\{j : 2^j\tilde{N}_m \geq \bar{N}_0\}$, and $N_0 = 2^k\tilde{N}_m$. Set $\tau_0 = \min\{C_1\epsilon_0^{1/2}, d(\epsilon_0, h)\}$.

(2) Set $k_0 = 0$. For $i \geq 1$, set $\epsilon_i = \epsilon_{i-1} + \tau_{i-1}$, and

$$\tau_i = \min\{1 - \epsilon_i, C_1\epsilon_i^{1/2}, d(\epsilon_i, h)\}. \tag{5.1}$$

If $\tau_i = 1 - \epsilon_i$, set $m = i$. The least admissible $N_i \geq C_2\epsilon_i^{-1/2}$ is so determined:

(i) If $k_{i-1} < k$, set $\bar{N}_i = \frac{N_{i-1}}{2}$. If $\bar{N}_i \geq C_2\epsilon_i^{-1/2}$, then set $k_i = k_{i-1} + 1$, $N_i = \bar{N}_i$; otherwise, set $k_i = k_{i-1}$, $N_i = N_{i-1}$.

(ii) If $k_{i-1} = k$, set $k_i = k_{i-1}$, $N_i = N_{i-1}$.

Remark 5.1 *By setting $k = 0$, $N_i = \tilde{N}_m$, $0 \leq i \leq m$, the meshing strategy above can be adapted to create a mesh for the radially symmetric solutions, for which orientation preserving adds no restrictions on N_i (see Theorem 3.3 and Remark 3.4). As a consequence, the total degrees of freedom of a dual-parametric bi-quadratic FE approximation are significantly less than that of an iso-parametric quadratic FE approximation, where the orientation preserving condition plays a leading role in determining N_i, especially when $\epsilon_i \ll h$ [20].*

Theorem 5.2 *Let u be a cavity solution satisfying the assumptions of Theorem 3.1. Then, for a given constant $C \geq (2-p)2^{p-1}$, there exists $0 < \hat{h} \leq \min\{\frac{2-p}{2^{2-p}C}, \frac{2-p}{2^{p-1}C}\}$ such that, for a reference mesh size $0 < h \leq \hat{h}$, on a mesh $\{\Omega_{(\epsilon_i,\tau_i)}\}_{i=0}^m$ with ϵ_i, τ_i, N_i produced by the above meshing strategy, we have $\det \nabla \Pi u(x) > 0$, and*

$$\|u - \Pi u\|_\infty = O(h^3), \tag{5.2}$$

$$\|u - \Pi u\|_{1,p} = O(h^2), \tag{5.3}$$

$$err(E(u; \Omega_{\epsilon_0})) = O(h^2). \tag{5.4}$$

Proof. The claims $\det \nabla \Pi u(x) > 0$, (5.2) and (5.3) follow from Theorem 3.1, Theorem 4.1 and Theorem 4.2 respectively, (5.4) is a direct consequence of (4.10) and $\sum_{i=0}^{m} A(\epsilon_i, \tau_i) = (2-p)\int_\epsilon^1 R^{1-p}dR \leq 1$. What remains to show is $N_i^{-1} = O(h)$, which is a consequence of $\tilde{N}_m \sim 1/h$ and $N_i \geq \tilde{N}_m$. ■

To estimate the total degrees of freedom, we need the following lemma.

Lemma 5.3 *Let* $f(x) = C_1 x^{1/2} + x - (x^{2-p} + Ch)^{\frac{1}{2-p}}$, $x \in [0,1]$, *where* $C_1 > 0$, $C > 0$ *and* $1 < p < 2$ *are given constants. Then, there exist positive constants* $a_1 < a_2$ *independent of* $h < \bar{h}_0 = \min\{\frac{(1+C_1)^{2-p}-1}{C}, \frac{(2-p)C_1}{C}(1+\frac{C}{s})^{\frac{1-p}{2-p}}\}$, *where* s *is the bigger root of the equation* $(2-p)C_1 x^2 - Cx - C^2 = 0$, *such that* $f(x) < 0$ *if* $x \in [0, a_1 h^{\frac{2}{2-p}}]$, *and* $f(x) \geq 0$ *if* $x \in [a_2 h^{\frac{2}{2-p}}, 1]$.

Proof. Since $x \geq 0$ and $1 < p < 2$, it follows that

$$f(x) \leq \bar{f}(x) = C_1 x^{1/2} + x - C^{\frac{1}{2-p}} h^{\frac{1}{2-p}},$$

thus, $f(x) < 0$, if $x < x_1 \triangleq 4\Big(\sqrt{C_1^2 + 4(Ch)^{\frac{1}{2-p}}} + C_1\Big)^{-2} C^{\frac{2}{2-p}} h^{\frac{2}{2-p}}$, which is the bigger root of $\bar{f}(x) = 0$.

For $x^{2-p} > sh$, it is easily verified that

$$\begin{aligned} f(x) &= C_1 x^{1/2} + x - x(1 + x^{p-2}Ch)^{\frac{1}{2-p}} \\ &= C_1 x^{1/2} + x - x(1 + \xi x^{p-2} Ch), \end{aligned}$$

where $\xi = \frac{1}{2-p}(1+\eta)^{\frac{p-1}{2-p}}$ and $0 < \eta < x^{p-2}Ch < Cs^{-1}$, thus, we have

$$f(x) > C_1 x^{1/2} - \frac{1}{2-p}(1 + Cs^{-1})^{\frac{p-1}{2-p}} Chx^{p-1}. \tag{5.5}$$

If $p \geq 3/2$, then $x^{p-1} \leq x^{1/2}$, hence $f(x) > (C_1 - \frac{1}{2-p}(1+Cs^{-1})^{\frac{p-1}{2-p}}Ch)x^{1/2} > 0$, since $h < \bar{h}_0$. If $p < 3/2$, then $\frac{p-1}{2-p} < 1$ and $x^{p-1}h < x^{2-p}x^{p-1}/s = x/s < x^{1/2}/s$, thus, it follows from (5.5) that

$$f(x) > \Big(C_1 - \frac{Cs^{-1}}{2-p}(1+Cs^{-1})^{\frac{p-1}{2-p}}\Big)x^{1/2} > \Big(C_1 - \frac{Cs^{-1}}{2-p}(1+Cs^{-1})\Big)x^{1/2}.$$

By the definition of s, this leads to $f(x) > 0$.

On the other hand, for $x^{2-p} \leq sh$, denoting $M = (C+s)^{\frac{1}{2-p}}$, we have

$$\begin{aligned} f(x) &= C_1 x^{1/2} + x - (Ch)^{\frac{1}{2-p}}(1 + x^{2-p}C^{-1}h^{-1})^{\frac{1}{2-p}} \\ &\geq C_1 x^{1/2} + x - (Ch)^{\frac{1}{2-p}}(1 + sC^{-1})^{\frac{1}{2-p}} \\ &= \tilde{f}(x) = C_1 x^{1/2} + x - Mh^{\frac{1}{2-p}}, \end{aligned}$$

Hence $f(x) \geq 0$, if $x \geq x_2 \triangleq 4M^2\Big(C_1 + \sqrt{C_1^2 + 4Mh^{\frac{1}{2-p}}}\Big)^{-2} h^{\frac{2}{2-p}}$, which is the bigger root of the equation $\tilde{f}(x) = 0$. The proof is completed by taking $a_1 = 4\Big(\sqrt{C_1^2 + 4C^{\frac{1}{2-p}}} + C_1\Big)^{-2} C^{\frac{2}{2-p}}$ and $a_2 = M^2 C_1^{-2} = (C+s)^{\frac{2}{2-p}} C_1^{-2}$. ■

Theorem 5.4 *Let $C_1 > 0$, $C_2 > 0$, $1 < p < 2$ and $C \geq (2-p)2^{p-1}$ be given. Let $a_1 < a_2$, $\bar{h}_0$ and $\hat{h}$ be the constants given in Lemma 5.3 and Theorem 5.2 respectively. For given $\epsilon_0 < 1$, let $\{\epsilon_i, \tau_i, N_i\}_{i=0}^m$ be defined by the meshing strategy with $h < \bar{h}_1 = \min\{\bar{h}_0, \hat{h}, C_1^{2-p} a_1^{1-p/2}(a_2-a_1)^{p-2}, C a_2^{p-2}\}$. Then, we have*

$$m \leq M_2 = \begin{cases} \left[\log_2 \log_{b(h)} \epsilon_0 C_1^{-2}\right] + 3 + [(Ch)^{-1}], & \text{if } a_2 h^{\frac{2}{2-p}} \geq \epsilon_0; \\ [(Ch)^{-1}], & \text{otherwise,} \end{cases} \tag{5.6}$$

$$m \geq M_1 = \frac{1 - \max\{\epsilon_0^{2-p}, a_2^{2-p} h\}}{Ch} - 1, \tag{5.7}$$

where $b(h) = a_1 C_1^{-2} h^{\frac{2}{2-p}}$. Consequently, the total degrees of freedom N_d satisfies

$$\tilde{N}_m M_1 \leq N_d \leq N_0 M_2, \tag{5.8}$$

where N_0 and $\tilde{N}_m$ are given as in the meshing strategy (1).

Proof. By Lemma 5.3, $C_1 x^{1/2} < d(x,h)$ if $x \leq a_1 h^{\frac{2}{2-p}}$, and $C_1 x^{1/2} \geq d(x,h)$ if $x \geq a_2 h^{\frac{2}{2-p}}$. Hence, by (5.1), $\epsilon_{i+1} = \epsilon_i + C_1 \epsilon_i^{1/2}$ if $\epsilon_i \leq a_1 h^{\frac{2}{2-p}}$, and $\epsilon_{i+1} = \epsilon_i + d(\epsilon_i, h)$ if $\epsilon_i \geq a_2 h^{\frac{2}{2-p}}$. Let ϵ_{m_1} be the biggest ϵ_i such that $\epsilon_i \leq a_1 h^{\frac{2}{2-p}}$, then for all $i \leq m_1$, $\epsilon_{i+1} = \epsilon_i + C_1 \epsilon_i^{1/2}$. Since $\epsilon_{m_1} = \epsilon_{m_1-1} + C_1 \epsilon_{m_1-1}^{1/2} > C_1 \epsilon_{m_1-1}^{1/2} > C_1^{1+1/2} \epsilon_{m_1-2}^{1/2^2} > \cdots > C_1^{1+1/2+\cdots+1/2^{m_1-1}} \epsilon_0^{1/2^{m_1}} = C_1^2 (\frac{\epsilon_0}{C_1^2})^{1/2^{m_1}}$. Let j be the smallest integer i such that $C_1^2 (\frac{\epsilon_0}{C_1^2})^{1/2^i} \geq a_1 h^{\frac{2}{2-p}}$, then $m_1 \leq j$. By the definition of j, one has

$$m_1 \leq j = \begin{cases} \log_2 \log_{b(h)} \frac{\epsilon_0}{C_1^2}, & \text{if } \log_2 \log_{b(h)} \frac{\epsilon_0}{C_1^2} \text{ is an integer;} \\ \left[\log_2 \log_{b(h)} \frac{\epsilon_0}{C_1^2}\right] + 1, & \text{otherwise.} \end{cases} \tag{5.9}$$

Let ϵ_{m_2} be the smallest ϵ_i such that $\epsilon_i \geq a_2 h^{\frac{2}{2-p}}$, then, for all $m_2 \leq i < m$, $\epsilon_{i+1}^{2-p} = \epsilon_i^{2-p} + Ch = \epsilon_{m_2}^{2-p} + C(i+1-m_2)h$. It follows from the facts that $\epsilon_{m+1} = 1.0$ and $\tau_m = \min\{1-\epsilon_m, d(\epsilon_m, h), C_1 \epsilon_m^{1/2}\}$ that m is the smallest integer j such that $\epsilon_j^{2-p} + Ch = \epsilon_{m_2}^{2-p} + C(j+1-m_2)h \geq 1$. Hence

$$m = \begin{cases} m_2 - 1 + \frac{1-\epsilon_{m_2}^{2-p}}{Ch}, & \text{if } \frac{1-\epsilon_{m_2}^{2-p}}{Ch} \text{ is an integer;} \\ m_2 + \left[\frac{1-\epsilon_{m_2}^{2-p}}{Ch}\right], & \text{otherwise.} \end{cases} \tag{5.10}$$

Next, we estimate $m_2 - m_1$. By the definition of m_1, $\epsilon_{m_1+1} = \epsilon_{m_1} + C_1 \epsilon_{m_1}^{1/2} > a_1 h^{\frac{2}{2-p}}$. Thus, $\tau_{m_1+2} \geq \min\{C_1 a_1^{\frac{1}{2}} h^{\frac{1}{2-p}}, d(\epsilon_{m_1+1}, h)\}$. This implies $\epsilon_{m_1+2} > \min\{C_1 a_1^{1/2} h^{\frac{1}{2-p}}$

$+a_1 h^{\frac{2}{2-p}}, (Ch)^{\frac{1}{2-p}}\}$. Hence, by the definition of $\bar{h}_1$, $\epsilon_{m_1+2} > a_2 h^{\frac{2}{2-p}}$. Consequently, by the definition of ϵ_{m_2}, we conclude $m_2 \le m_1 + 2$, which together with (5.9) and (5.10) yields (5.6).

If $\epsilon_0 \ge a_2 h^{\frac{2}{2-p}}$, then (5.7) follows directly from (5.10), since in this case $m_2 = 0$. If $\epsilon_0 < a_2 h^{\frac{2}{2-p}}$, then $m_2 \ge 1$ and $\epsilon_{m_2-1} < a_2 h^{\frac{2}{2-p}}$ by the definition of m_2. Thus, for all $m_2 \le i \le m$, $\epsilon_i^{2-p} = \epsilon_{m_2}^{2-p} + C(i - m_2)h \le \epsilon_{m_2-1}^{2-p} + C(i + 1 - m_2)h$. Set

$$j_0 = \begin{cases} m_2 - 2 + \frac{1-\epsilon_{m_2-1}^{2-p}}{Ch}, & \text{if } \frac{1-\epsilon_{m_2-1}^{2-p}}{Ch} \text{ is an integer;} \\ m_2 - 1 + \left[\frac{1-\epsilon_{m_2-1}^{2-p}}{Ch}\right], & \text{otherwise.} \end{cases} \tag{5.11}$$

Then, it is easily verified that $\epsilon_i < 1$, for all $i \le j_0$. Hence, by the definition of m, we conclude $m \ge j_0$, which implies (5.7), since $m_2 \ge 1$ and $\epsilon_{m_2-1} < a_2 h^{\frac{2}{2-p}}$. ■

It is worth noticing that there are two solution dependent constants C_1 and C_2, which are not known a priori, used in the meshing strategy. In applications, we can always start with $C_1 := d(\epsilon_0, h)\epsilon_0^{-1/2}$ and $C_2 := \tilde{N}_m \epsilon_0^{1/2}$, which are the least C_1 and greatest C_2 such that the orientation preserving conditions will practically not affect the mesh produced. It is of vital importance to know what would happen if the constants are not properly given, and how to adjust the mesh in an a posteriori fashion so that the conditions C1-C4 are satisfied in the end. To specify this, we present below two examples in both radially symmetric and nonsymmetric cases, where the energy density is given by (1.6) with $p = 3/2$, $\omega = 2/3$, and $g(x) = 2^{-1/4}(\frac{1}{2}(x-1)^2 + \frac{1}{x})$, and we take $A = A_1 = A_2 = 0.8$, $h = 0.05$.

C_1	ϵ_1	ϵ_2	ϵ_3	ϵ_4	ϵ_5	ϵ_6	ϵ_7	ϵ_8	ϵ_9
1	0.0101	0.0402	0.0903	0.1604	0.2505	0.3606	0.4907	0.6408	0.8109
0.9	0.0091	0.0382	0.0873	0.1563	0.2454	0.3545	0.4836	0.6327	0.8017

Table 1: Radially symmetric case: $\epsilon_0 = 0.0001$, $N_i = 16$, $\epsilon_{10} = 1.0$.

Example 5.5 *In the radially symmetrical case, let* $\epsilon_0 = 0.0001$, $u_0(x) = 2x$, *and* $N_i = N_h = A/h$. *For* $C = 2$, $C_1 = 1.0$ *and* 0.9, *the mesh strategy produces two meshes shown in Table 1. While the numerical solutions obtained on both meshes successfully capture the cavitation, the solution with* C_1 *a marginally too big fails*

to be orientation preserving. In fact, $\det \nabla u_h(x) < 0$ *is detected on the element vertices on the inner boundary* $\{x : |x| = \epsilon_0\}$*, where the orientation preserving is found most easily broken. Our numerical experiments show that, whenever this happens, instead of reducing* C_1*, a proper mesh can be obtained simply by dividing the inner most layer into two, repeat if necessary, according to the condition (C3).*

Example 5.6 *Let* $\epsilon_0 = 0.0005$ *and* $u_0(x) = (2.5x_1, 2x_2)^T$*, then, the corresponding cavity solution is non-radially-symmetric. Now, we are facing the problem of choosing* C_1 *and* C_2 *appearing in the conditions* $\tau \leq C_1\epsilon^{1/2}$ *and* $N \geq C_2\epsilon^{-1/2}$*. For* $C = 3$*,* $C_1 = 1.0$ *and,* $C_2 = 1.1$*, the meshing strategy produces a mesh shown in "Test 1" in Table 2, where* $N_i = N_0/2$*,* $\forall i \geq 1$*, which holds also for other three tests. It turns out that the numerical solution obtained on this mesh is indeed orientation preserving. While for* $C_1 = 1.25$ *(see Test 2) or* $C_2 = 0.9$ *(see Test 3), the numerical solutions obtained on the corresponding meshes will fail to be orientation preserving. Again, it is found that the failure is most likely to happen on the element vertices on the inner boundary of the domain* Ω_{ϵ_0}*. And again, instead of reducing* C_1 *or increasing* C_2*, a proper mesh can usually be obtained simply by dividing the inner most layer into two (see Test 4 where* $\epsilon_8 = 1.0$*), according to the condition (C3), or doubling* N_0*, or both, and repeat the process if necessary.*

Test	ϵ_1	ϵ_2	ϵ_3	ϵ_4	ϵ_5	ϵ_6	ϵ_7	N_0	Result
1	0.0229	0.0907	0.2036	0.3614	0.5643	0.7946	1.0	50	Succeed
2	0.0285	0.1016	0.2198	0.3829	0.5911	0.8442	1.0	50	Fail
3	0.0229	0.0907	0.2036	0.3614	0.5643	0.7946	1.0	40	Fail
4	0.0091	0.0285	0.1016	0.2198	0.3829	0.5911	0.8442	50	Succeed

Table 2: Non-radially-symmetric case: $\epsilon_0 = 0.0005$, $u_0(x) = (2.5x_1, 2x_2)^T$.

Remark 5.7 *In our code, the condition* $\det \nabla u_h > 0$ *is firstly only checked on quadrature nodes in a gradient flow iteration; after the iteration converges, the condition* $\det \nabla u_h > 0$ *is checked on elements vertices, particulary those on the inner boundary of the domain* Ω_{ϵ_0}*, where the condition is most easily be broken;*

the mesh layer, where $\det \nabla u_h < 0$ *is detected, is then refined accordingly. Such a modified meshing strategy practically makes the whole process more efficient, though a mesh so obtained is not necessarily "optimal".*

6 Numerical experiments and results

In our numerical experiments, the energy density is given by (1.6) with $p = 3/2$, $\omega = 2/3$, and $g(x) = 2^{-1/4}(\frac{1}{2}(x-1)^2 + \frac{1}{x})$, the domain $\Omega_{\epsilon_0} = B_1(0) \setminus B_{\epsilon_0}(0)$ with a displacement boundary $\Gamma_0 = \partial B_1(0)$ and a traction free boundary $\Gamma_1 = \partial B_{\epsilon_0}(0)$, and the meshes used are shown in Table 3 and Table 4, which are produced by the meshing strategy with $C = 2$, $C_1 = 0.9$, $A = 0.8$ for $\epsilon_0 = 0.01$, $\epsilon_0 = 0.0001$ and various h, and it happens that, in all these meshes, $N_i = N_h = A/h$ on each of the $m+1$ mesh layers. Figure 3 shows that the total degrees of freedom N_d is basically a quadratic function of h^{-1}.

h	$\min \tau_i$	$\max \tau_i$	m	N_h
0.04	0.0224	0.1504	11	20
0.03	0.0156	0.1164	14	30
0.02	0.0096	0.0768	22	40
0.01	0.0044	0.0396	44	80
0.005	0.0021	0.0199	89	160

Table 3: $\epsilon_0 = 0.01$.

h	$\min \tau_i$	$\max \tau_i$	m	N_h
0.04	0.008	0.1488	12	20
0.03	0.0048	0.1128	16	30
0.02	0.0024	0.076	24	40
0.01	0.0008	0.0392	49	80
0.005	0.0003	0.0197	98	160

Table 4: $\epsilon_0 = 0.0001$.

6.1 Radially symmetric case with $u(x)|_{\Gamma_0} = \lambda x$

The convergence behavior of the radially symmetric numerical cavity solutions corresponding to $\lambda = 2.0$ obtained by the dual-parametric bi-quadratic FEM are shown in Figure 4-Figure 6, where the high precision numerical solutions to the equivalent 1-D ODE problem are taken as the exact solutions [2, 10].

Figure 4 shows that the energy error $|E(u) - E(u_h)| = O(N_d^{-2}) = O(h^4)$, which is even better than our energy error estimate on the interpolation function (see

(5.4)). In Figure 5 and Figure 6, it is shown that $\|u-u_h\|_{0,2} = O(N_d^{-3/2}) = O(h^3)$ and $\|u-u_h\|_{1,p} = O(N_d^{-1}) = O(h^2)$ respectively, which are in good agreement with our interpolation error estimates (see (5.2) and (5.3)).

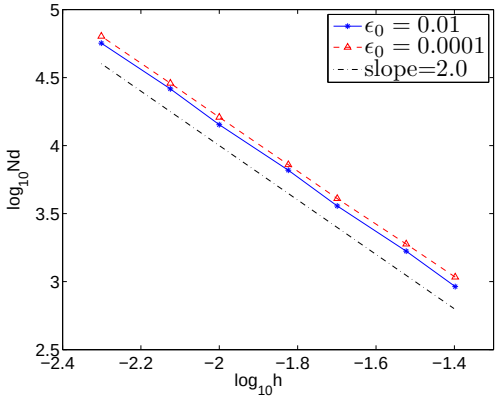

Figure 3: $N_d \sim Kh^{-2}$.

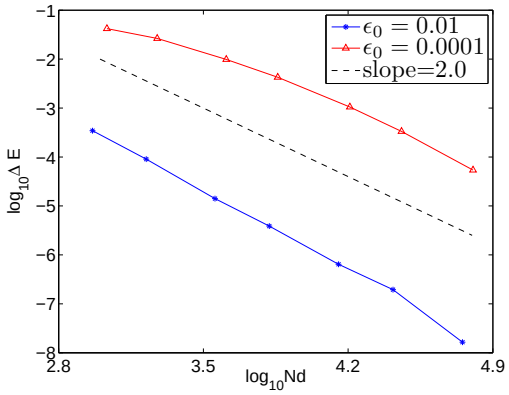

Figure 4: The energy error.

A comparison between $W^{1,p}$ errors of the iso-parametric triangular FEM ([20]) and the dual-parametric bi-quadratic FEM is also shown in Figure 6, which demonstrates that the latter should be a more efficient method in cavitation computation.

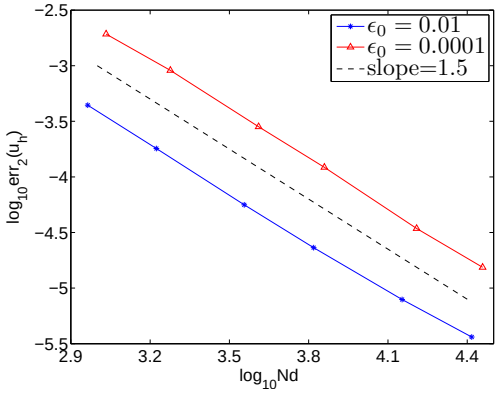

Figure 5: The L^2 errors of u_h.

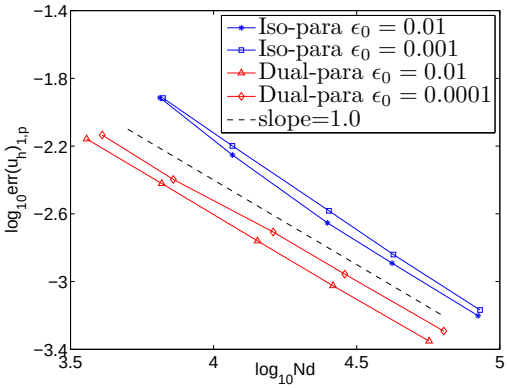

Figure 6: The $W^{1,p}$ errors of u_h.

6.2 Non-radially-symmetric case with $u(x)|_{\Gamma_0} = (\lambda_1 x_1, \lambda_2 x_2)^T$

The numerical results for $\lambda_1 = 2.5$, $\lambda_2 = 2.0$, $\epsilon_0 = 0.01$ obtained on the mesh given in Table 3 are shown in Figure 7-Figure 10.

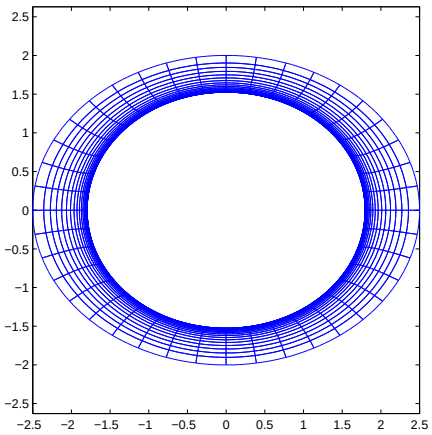

Figure 7: The numerical solution.

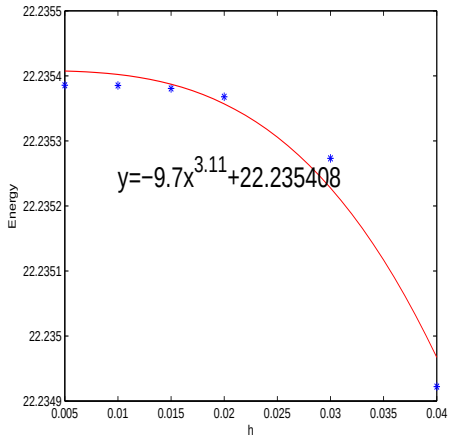

Figure 8: Convergence of the energy.

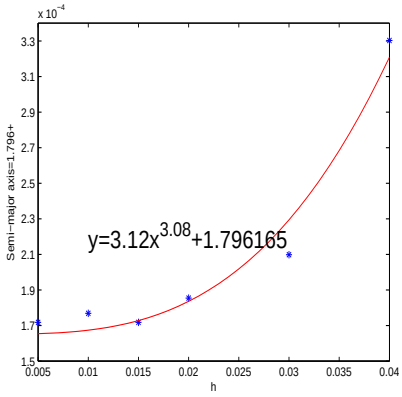

(a) Convergence of semi-major axis.

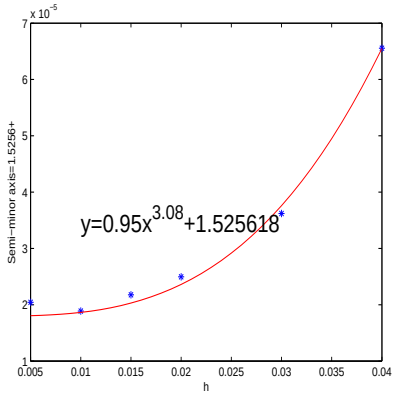

(b) Convergence of semi-minor axis.

Figure 9: The convergence behavior of the cavity of u_h.

Figure 7 shows the numerical solution with $h = 0.02$, where the cavity is seen to be approximately an ellipse. The convergence behaviors of the energy, semi-major axis, and semi-minor axis of the cavity, with respect to the mesh size h, are displayed respectively in Figure 8, Figure 9(a) and Figure 9(b). The convergence behavior of $\|u_h - u_{h/2}\|_{0,2}$ and $|u_h - u_{h/2}|_{1,p}$, in terms of $N_d \sim h^{-2}$, are demonstrated respectively in Figure 10(a) and Figure 10(b). The numerical results are clearly in good agreement with our analytical results (see (5.2)-(5.4)).

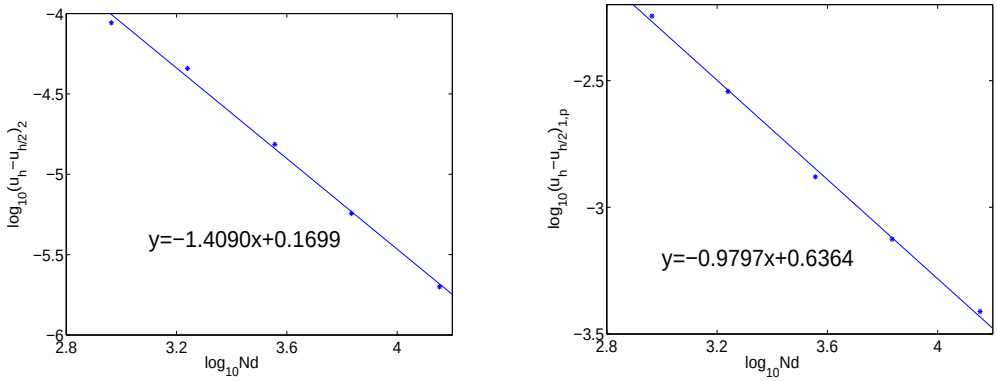

(a) Error in L^2 norm.

(b) Error in $W^{1,p}$ norm.

Figure 10: The convergence behavior of $\|u_h - u_{h/2}\|$.

7 Concluding remarks

We derived the orientation preserving conditions and interpolation errors of the dual-parametric bi-quadratic rectangular FEM for both radially symmetric and general non-symmetric cavity solutions, which is the first theoretical result of its kind in this field, and established an optimal meshing strategy for the method in computing void's growth based on an error equi-distribution principle. Numerical results obtained on the meshes produced by our meshing strategy verified the efficiency of the method. In fact, our numerical experiments showed that the convergence rates of the finite element cavitation solutions are in good agreement with our interpolation error estimates, and the total degrees of freedom needed for the method to achieve a given level of approximation accuracy is of an optimal order, and is much less than that of the iso-parametric quadratic triangular FEM in practical cavitation computation.

References

[1] Bai, Y., Li, Z., Numerical solution of nonlinear elasticity problems with laurentiev phenomenon. **Math. Models Meth. Appl. Sci., 17** (2007), 1619-1640.

[2] Ball, J.M., Discontinuous equilibrium solutions and cavitation in nonlinear elasticity. **Philos. Trans. R. Soc. London, A 306** (1982), 557-611.

[3] Ball, J.M., Knowles, G., A numerical method for detecting singular minimizers. **Numer. Math., 51** (1987), 181-197.

[4] Gent, A.N., Lindley, P.B., International rupture of bounded rubber cylinders in tension. **Proc. R. Soc. London., A 249** (1958), 195-205.

[5] Henao, D., Cavitation, invertibility, and convergence of regularized minimizers in nonlinear elasticity. **J. Elast., 94** (2009), 55-68.

[6] Horgan, C.O., Polignone, D.A., Cavitation in nonlinearly elastic solids: a review. **Appl. Mech. Rev., 48(8)** (1995), 471-485.

[7] Lavrentiev, M., Sur quelques problems du calcul des variations. **Ann. Math. Pure Appl., 4** (1926), 7-28.

[8] Li, Z., A numerical method for computing singular minimizers. **Numer. Math., 71** (1995), 317-330.

[9] Lian, Y., Li, Z., A dual-parametric finite element method for cavitation in nonlinear elasticity. **J. Comput. Appl. Math., 236** (2011), 834-842.

[10] Lian, Y., Li, Z., A numerical study on cavitations in nonlinear elasticity-defects and configurational forces. **Math Models Meth. Appl. Sci., 21** (2011), 2551-2574.

[11] Lian, Y., Li, Z., Position and size effects on voids growth in nonlinear elasticity. **Int. J. Fracture, 173** (2012), 147-161.

[12] Müller, S., Spector, S.J., An existence theory for nonlinear elasticity that allows for cavitation. **Arch. Rat. Mech. Anal., 131** (1995), 1-66.

[13] Negrón-Marrero, P.V., A numerical method for detecting singular minimizers of multidimensional problems in nonlinear elasticity. **Numer. Math., 58** (1990), 135-144.

[14] Negrón-Marrero, P.V., Betancourt, O., The numerical computation of singular minimizers in two-dimensional elasticity. **J. Comput. Phys., 113** (1994), 291-303.

[15] Sivaloganathan, J., Uniqueness of regular and singular equilibia for spherically symmetric problems of nonlinear elasticity, **Arch. Rat. Mech. Anal., 96** (1986), 97-136.

[16] Sivaloganathan, J., Spector. S.J., Tilakraj. V., The convergence of regularized minimizers for cavitation problems in nonlinear elasticity. **SIAM J. Appl. Math., 66** (2006), 736-757.

[17] Sivaloganathan, J., Spector, S. J., On the existence of minimisers with prescribed singular points in nonlinear elasticity. **J. Elast., 59** (2000), 83-113.

[18] Sivaloganathan, J., Spector, S. J., On the optimal location of singularities arising in variational problems in nonlinear elasticity. **J. Elast., 58** (2000), 191-224.

[19] Sivaloganathan, J., Spector, S. J., On cavitation, configurational forces and implications for fracture in a nonlinearly elastic material. **J. Elast., 67** (2002), 25-49.

[20] Su, C., Li, Z., Orientation preserving conditions and errors of a FEM in cavitation computation in nonlinear elasticity. Research report 2014-001, LMAM & School of Mathematical Sciences, Peking University.

[21] Stuart, C. A., Radially symmetric cavitation for hyperelastic meterials. **Ann. Inst. Henri Poincaré, 2**(1985), 251-263.

[22] Xu, X., Henao, D., An efficient numerical method for cavitation in nonlinear elasticity. **Math Models Meth. Appl. Sci., 21** (2011), 1733-1760.